THE JOURNAL OF BIOLOGICAL CHEMISTRY
Vol. 277, No. 52, Issue of December 27, pp. 50636–50642, 2002
Printed in U.S.A.

Knock-down of the Type 3 Ryanodine Receptor Impairs Sustained Ca^{2+} Signaling via the T Cell Receptor/CD3 Complex*

Received for publication, September 5, 2002, and in revised form, September 19, 2002
Published, JBC Papers in Press, September 26, 2002, DOI 10.1074/jbc.M209061200

Nadine Schwarzmann, Svenja Kunerth, Karin Weber, Georg W. Mayr, and Andreas H. Guse‡

From the University Hospital Hamburg-Eppendorf, Center for Theoretical Medicine, Institute for Cellular Signal Transduction, Martinistr. 52, D-20246 Hamburg, Germany

In Jurkat T cells, the type 3 ryanodine receptor (RyR) was knocked-down by stable integration of plasmid expressing type 3 ryanodine receptor antisense RNA. Stable integration of the antisense plasmid in individual clones was demonstrated by PCR of genomic DNA, expression of antisense RNA by reverse transcriptase PCR, and efficiently reduced expression of type 3 ryanodine receptor protein by Western blot. Selected clones were successfully used to analyze T cell receptor/CD3 complex-mediated Ca^{2+} signaling. Reduced expression of the type 3 RyR resulted in (i) significantly decreased Ca^{2+} signaling in the sustained phase and (ii) in permeabilized cells in a significantly impaired response toward cyclic ADP-ribose but not to D-*myo*-inositol 1,4,5-trisphosphate. For the first time, the role of the type 3 RyR in sustained Ca^{2+} signaling was directly visualized by confocal Ca^{2+} imaging as a significant contribution to the number and the magnitude of subcellular Ca^{2+} signals. These data suggest that the type 3 ryanodine receptor is essential in the sustained Ca^{2+} response in T cells.

Ca^{2+} signaling by ligation of the T cell receptor (TCR)/CD3[1] complex is a complicated process involving the formation and breakdown of the second messengers D-*myo*-inositol 1,4,5-trisphosphate (IP_3) and cyclic adenosine diphosphoribose (cADPR) in a temporally coordinated fashion (1–3). In addition to IP_3 and cADPR, nicotinic acid adenine dinucleotide phosphate (NAADP) is an essential regulator of T cell Ca^{2+} signaling (4), although the exact role of this nucleotide has not yet been clarified. Jurkat T cells preincubated with the specific, membrane-permeant cADPR antagonist 7-deaza-8-Br-cADPR (5) showed characteristic defects in the onset and in the long-lasting phase of TCR/CD3- and β_1-integrin-mediated Ca^{2+} signaling (2, 6). In addition, in peripheral human T cells, 7-deaza-8-Br-cADPR efficiently blocked expression of the activation antigens CD25 and MHCII and blocked proliferation upon CD3 ligation (2). These data suggested that cADPR plays an essential role in the sustained phase of T cell Ca^{2+} signaling. Although the molecular target for cADPR is still a controversial issue (reviewed in Ref. 7), in many cell systems, the pharmacology of cADPR-mediated Ca^{2+} release points strongly toward ryanodine receptors (RyR) as the intracellular Ca^{2+} channels involved (Ref. 8 and reviewed in Ref. 9).

In T cells, expression of the RyR has been demonstrated by [^{3}H]ryanodine binding (2, 10, 11), Western blot analysis (2, 10, 12), and immunohistochemical staining (10, 12). Ca^{2+} signaling activated by caffeine, ryanodine, and/or suramin also provided evidence for a functional role of RyR in T cells (11, 13, 14). Inhibition of cADPR-mediated Ca^{2+} release by ruthenium red and high Mg^{2+} concentrations in permeabilized T cell preparations indicate an involvement of RyR in cADPR-mediated Ca^{2+} release (15, 16).

From our kinetic and pharmacological data, we have hypothesized recently that one of the essential Ca^{2+} release events in the sustained phase of TCR/CD3-activated Ca^{2+} signaling is cADPR-mediated release of Ca^{2+} via RyR (17). To directly prove the involvement of RyR in this phase, we intended to knock-down the type 3 RyR by an antisense RNA approach; the type 3 RyR was chosen because it appeared to be the major isoform of RyR in Jurkat T cells (2, 18). Antisense approaches have recently been successfully used to demonstrate the importance of the type 1 receptor for IP_3 (IP_3R) in Jurkat T cells (19) or the role of types 1 and 2 RyR in Ca^{2+}-induced Ca^{2+} release (CICR) in portal vein myocytes (20). Although the mechanisms underlying antisense approaches are under intense discussion (21–25), the successful study by Jayaraman *et al.* (19) in Jurkat T cells prompted us to establish Jurkat subclones with stable integration of a type 3 RyR antisense construct.

EXPERIMENTAL PROCEDURES

Materials—Fetal calf serum (tetracyclin-free) was obtained from Biochrom (Berlin, Germany). Primers were purchased from MWG Biotech (Ebersberg, Germany). Chemicals were obtained at highest quality available from Mallinckrodt Baker (Griesheim, Germany), Merck, Sigma, Biomol (Hamburg, Germany), Serva (Heidelberg, Germany), FMC Bioproducts, Biozym (Hessisch Oldendorf, Germany), PeqLab (Erlangen, Germany), or Applichem (Darmstadt, Germany).

Cell Culture— Tet-On Jurkat T cells stably transfected with the regulatory pTet-On plasmid were obtained from Clontech. The cells were cultured in RPMI 1640 supplemented with Glutamax I, 10% (v/v) fetal calf serum (free of tetracyclin, Biochrom), 25 mM Hepes, 100 units/ml penicillin, 50 μg/ml streptomycin, and 100 μg/ml G418-Sulfat (termed "complete" RPMI 1640 medium later on). Culturing was done at 37 °C in a humidified atmosphere at 5% CO_2 in air.

Preparation of Plasmids and Transfection—Total RNA was prepared from Jurkat T cells using Tri-reagent (Sigma), and a 511-bp fragment specific for the human type 3 RyR was amplified by RT-PCR using the Titan one-Tube RT-PCR system (Roche Diagnostics) followed by a nested PCR step using *Pfu* Turbo DNA polymerase (Stratagene, La Jolla, CA) and the following pairs of primers: GTG AAG AGG AAT GTC ACC/CAA CCT TCT GAC CAC ACC (forward PCR/reverse PCR) and

* This work was supported by grants from the Deutsche Forschungsgemeinschaft (GU 360/2-4 and 2-5 to A. H. G. and to G. W. M.), the Deutsche Akademische Austauschdienst (VIGONI-program Grant 314-vigoni-dr to A.H.G.), the Forschungsförderungsfonds of the Medical Faculty (Grant F-408-1 to A. H. G.), and the Wellcome Trust (Research Collaboration Grants 51326 and 068065 to A. H. G.). The costs of publication of this article were defrayed in part by the payment of page charges. This article must therefore be hereby marked "*advertisement*" in accordance with 18 U.S.C. Section 1734 solely to indicate this fact.

‡ To whom correspondence should be addressed. Tel.: 49-40-42803-2828; Fax: 49-40-42803-9880; E-mail: guse@uke.uni-hamburg.de.

[1] The abbreviations used are: TCR/CD3, T cell receptor/CD3; cADPR, cyclic adenosine diphosphoribose; CICR ,Ca^{2+}-induced Ca^{2+} release; EGFP, enhanced green fluorescent protein; IP_3, D-*myo*-inositol 1,4,5-trisphosphate; IP_3R, IP_3 receptor; RISC, RNA-induced silencing complex; RT-PCR, reverse transcriptase PCR; RyR, ryanodine receptor.

CTA AAG CTT TCC AGT TGC TCT TCA CCA TCC/CTA GGA TCC CAC AGG TAC TCA GCT TGC TCC (forward nested PCR/reverse nested PCR). The 250-bp control fragment was amplified from pEGFP-N1 (Clontech) using the following pairs of primers: TGA AGT TCG AGG GCG GAC ACC/GTG ATC GCG CTT CTC GTT GG (forward PCR/reverse PCR) and CTA AAG CTT TGG TGA ACC GCA TCG AGC/CTA GGA TCC CTC AGG TAG TGG TTG TCG (forward nested PCR/reverse nested PCR). The amplicons were digested using *Bam*HI and *Hin*dIII and cloned in reverse (antisense) orientation into the eukaryotic expression vector pTRE2 (Clontech). The identity of the inserts was checked by automated DNA sequencing.

Before transfection of Tet-On Jurkat cells, the plasmids were linearized using *Aat*II (pTRE2 plasmids) and *Hin*dIII (selection plasmid pTK-Hyg), purified by phenol-chloroform extraction, and dissolved in sterile water. Transfection was done by electroporation of 2×10^7 cells in 400 μl of medium using 40 μg of pTRE2 plasmids plus 2 μg of pTK-Hyg; electroporation parameters were 0.2 kV of voltage and 960 microfarads of capacity. The cells were then left in the electroporation cuvette for another 20 min and then resuspended in 10 ml of complete RPMI 1640 medium and cultured.

Cloning Procedure—At 48 h past electroporation, hygromycin-resistant cells were selected first in bulk culture. Hygromycin concentration was 50 μg/ml in the first week, then increased to 100 μg/ml for 3 days, again increased to 200 μg/ml for another 4 days, and then left at 50 μg/ml for another 2 weeks. Surviving cells were then subcloned using the limiting dilution procedure: cells were seeded at 0.3 cells/well in 96-well plates in complete RPMI 1640 medium additionally supplemented with 1 mM sodium pyruvate and 50 μg/ml hygromycin for 4 weeks. Surviving clones were then expanded in the same medium.

PCR of Genomic DNA—Stable integration of pTRE2 plasmids was analyzed by genomic PCR (500 ng of template DNA, 40 cycles) after preparation of genomic DNA from each individual clone using the Invisorb® Cell DNA Mini HTS 96-Kit/V (Invitek, Crispin Biomedical Supply, Houston, TX) according to the manufacturer's instructions. The forward primer (AGA GCT CGT TTA GTG AAC CG) was specific for a portion of the promoter region of pTRE2, and the reverse primer (CTC ACC CTG AAG TTC TCA GC) was specific for the multiple cloning site of pTRE2, thereby spanning a 208-bp fragment for pTRE, a 681-bp fragment for pTRE-511, and a 420-bp fragment for pTRE-EGFP.

RT-PCR—Total RNA was prepared from all clones with stable integration of pTRE2 plasmids using the RNeasy-Kit (Qiagen, Hilden, Germany) and on-column DNase digest according to the manufacturer's instructions. Primers were designed as follows. The forward primers for the different pTRE2 plasmids (pTRE2-511, CTA GGA TCC CAC AGG TAC TCA GCT TGC TCC; pTRE2-EGFP, CTA GGA TCC CTC AGG TAG TGG TTG TCG) both recognized a specific region within the 5′-end of the insert, whereas the reverse primer was specific for the polyadenylation site of pTRE2 (CTC ACC CTG AAG TTC TCA GC). Thus, the expected amplicon sizes were different from endogenous RNA.

Preparation of Subcellular Fractions—Subcellular fractions were prepared from the different Tet-On Jurkat clones as described in previous publications (2, 33).

SDS-PAGE and Western Blot—P10 membranes (50 μg of protein/lane) were subjected to reducing SDS-PAGE on a 6% separation gel (3% stacking gel) as detailed earlier (2). Protein transfer to nitrocellulose membrane was carried out by tank blotting at 7 mA/cm^2 (total of 400 mA) for 3 h at 10 °C. Unspecific binding to the membrane was then blocked by 5% (w/v) dry milk powder in Tris-buffered saline/Tween 20 at room temperature for 45 min. Immunostaining was done with anti-RyR_{common} and anti-IP_3R_{common} monoclonal antibodies (Calbiochem and BD Biosciences-Transduction Laboratories) incubated overnight in 2.5% (w/v) dry milk powder in Tris-buffered saline/Tween 20 at 10 °C with repeated rinsing and a further 1-h incubation using horseradish peroxidase-conjugated goat anti-mouse antiserum. Then, the membranes were washed by a complex protocol and developed using the ECL system (Amersham Biosciences) according to the manufacturer's instructions.

Determination of Intracellular Ca^{2+} Concentration—Tet-On Jurkat T cell clones were loaded with Fura2/AM as described (13). $[Ca^{2+}]_i$ was determined in aliquots of 1.5×10^6 Fura2-loaded cells in a Hitachi F-2000 spectrofluorimeter operated in the ratio mode (alternating excitation wavelengths, 340 and 380 nm; emission wavelength, 495 nm). Each tracing was calibrated for the maximal ratio by addition of ionomycin (1 μM) and for the minimal ratio by addition of EGTA/Tris (4 mM/40 mM) at the end of each measurement.

Confocal Ca^{2+} Imaging—Confocal Ca^{2+} imaging was carried out exactly as will be published elsewhere[2] except that the period of image acquisition with maximal rate was done at a late point (at about 15 min). In brief, stacks of three images at 0.5 μm distance at each excitation wavelength (340 and 380 nm) were acquired using an Improvision system (Heidelberg, Germany) centered around an inverted microscope (Leica DMIRE2). Grayscale images were captured at 8 bits and 640 × 512 pixels using a Hamamatsu CCD camera (type ORCA ER C4742-95-ER). The stacks of three images at a given wavelength were then used to calculate a confocal image using the nearest neighbor algorithm of the Openlab software module "volume deconvolution" (Improvision). Finally, ratio images were constructed pixel-by-pixel, calibrated, and converted into pseudocolor images using the Openlab software modules "ratio" and "density calibration" (Improvision).

Determination of Ca^{2+} Release in Permeabilized Cells—Permeabilized cells were prepared, and $[Ca^{2+}]$ was determined in the presence of Fura2, ATP, an ATP-regenerating system in a Hitachi F-2000 spectrofluorimeter operated in the ratio mode as described recently (34). In brief, Tet-On Jurkat T cell clones (2×10^8 cells) were permeabilized by saponin (40 μg/ml, 22 min) in an intracellular buffer, washed, and left on ice for 2 h to allow for resealing of intracellular membrane vesicles. Then, aliquots of 3.3×10^7 cells were analyzed in the presence of 1 μM Fura2/free acid at alternating excitation wavelengths (340 and 380 nm) and at 495-nm emission wavelength. Loading of intracellular Ca^{2+} stores was performed in the presence of creatine kinase (final concentration, 20 units/ml), creatine phosphate (final concentration, 20 mM) and ATP (final concentration, 1 mM). Then, cADPR (10 μM), IP_3 (4 μM), and ionomycin (1 μM) were added successively. Finally, each tracing was calibrated for $[Ca^{2+}]$ by addition of 1 mM $CaCl_2$ and 4 mM EGTA/40 mM Tris.

RESULTS

To generate Jurkat T cell clones with reduced expression of the type 3 RyR, the Tet-On system (26) was used. Commercially available Jurkat T cells stably transfected with the regulatory pTet-On plasmid (Clontech) were further transfected by electroporation with the responsive plasmid pTRE2 (Clontech). The following cDNA fragments were cloned in antisense orientation into the plasmid pTRE2: a 511-bp cDNA fragment from the human type 3 RyR corresponding to base pairs 12657–13167 (NCRI nucleotide data base accession number NM_001036.1) of the type 3 RyR mRNA (pTRE2-511) and an irrelevant control 250-bp cDNA fragment from EGFP (pTRE2-EGFP). The cells were co-transfected with the hygromycin resistance plasmid pTK-Hyg to allow for hygromycin resistance selection.

After electroporation selection was first carried out in bulk culture and, after the death of the majority of cells (about 95%), stable, hygromycin-resistant clones were obtained by limiting dilution (for details, see "Experimental Procedures"). For the type 3 RyR antisense plasmid pTRE2-511, 57 clones out of 400 wells were obtained; for the control plasmid pTRE2-EGFP, 29 clones out of 266 wells were obtained. The clones were selected according to the following strategy: first, the stable integration of the plasmids into the genome of the Tet-On Jurkat T cells was analyzed by PCR of genomic DNA; secondly, expression of antisense mRNA was determined by RT-PCR; and thirdly, reduced expression of the type 3 RyR was checked by SDS-PAGE and Western blot.

PCR of genomic DNA was conducted 3 months after transfection, assuring that the plasmids were either stably integrated or degraded. PCR of genomic DNA data from a selection of individual clones (clones 21–41) demonstrates that a sufficient number of stably transfected clones for the type 3 RyR antisense plasmid pTRE2-511 was generated (Fig. 1*A*, *left panel*). Similarly, for the control plasmid pTRE2-EGFP and for vector-transfected cells (pTRE2), sufficient stably transfected clones were

[2] S. Kunerth, G. W. Mayr, F. Koch-Nolte, and A. H. Guse, unpublished data.

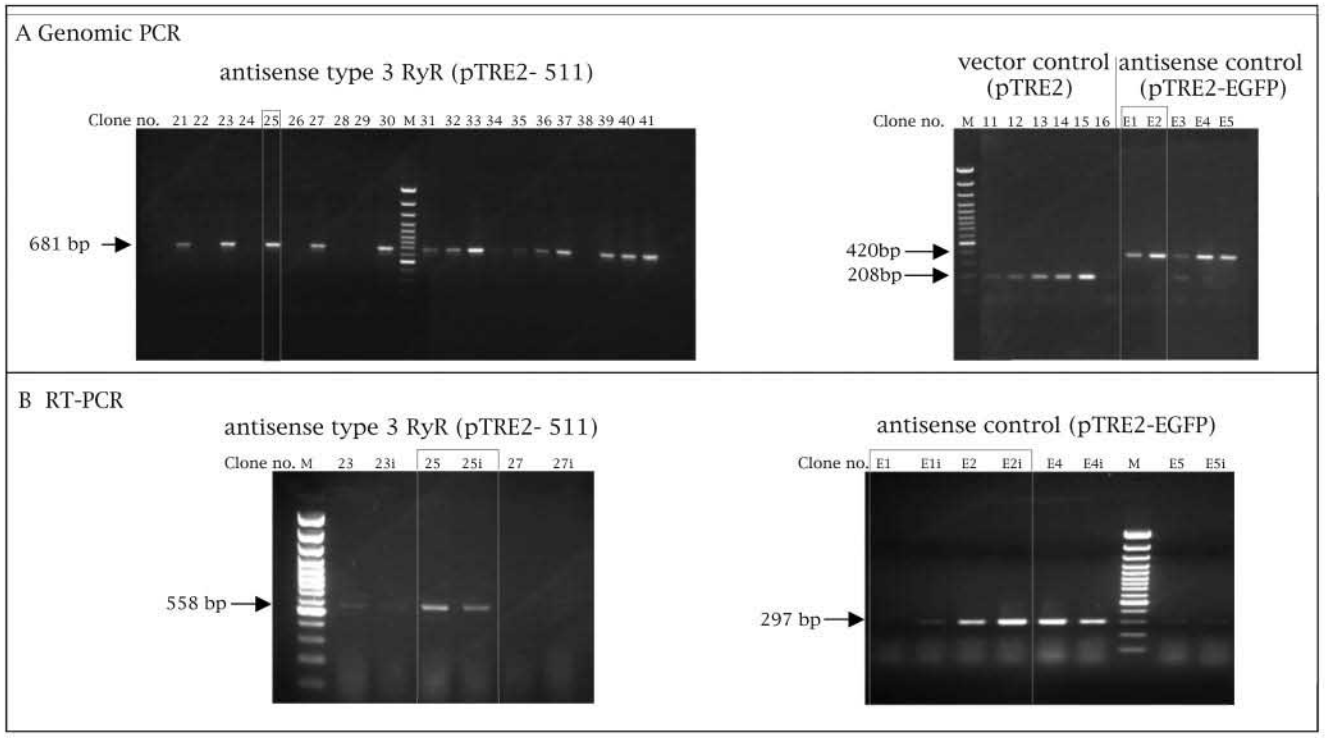

FIG. 1. **Genomic integration and mRNA expression of type 3 RyR antisense construct.** As shown in *A*, genomic integration of the type 3 RyR antisense plasmid pTRE2-511, the control plasmid pTRE2-EGFP, and the plasmid pTRE2 (without insert) was analyzed by genomic PCR using 500 ng of DNA as template and 40 cycles. Aliquots of the PCR reactions were then analyzed on a 2% agarose gel. The forward primer was localized in the promoter region of pTRE2, and the reverse primer was localized in the multiple cloning site of pTRE2. Expected amplicon sizes were 681 bp for pTRE2-511 (*left panel*), 208 bp for pTRE2, and 420 bp for pTRE2-EGFP (*right panel*). As shown in *B*, RT-PCR was performed using 500 ng of total RNA as template and 28 cycles. The forward primers were specific for the insert, whereas the reverse primer recognized a portion of the polyadenylation site of pTRE2. Aliquots of the RT-PCR reactions were then analyzed on a 2% agarose gel. Expected amplicon lengths were 558 bp for pTRE2-511 (*left panel*) and 297 bp for pTRE2-EGFP (*right panel*). Lanes marked with *i* indicate that the cells had been cultured with 1 μg/ml doxycyclin for 48 h before the preparation of RNA. Lanes marked with *M* indicate a 100-bp DNA ladder with a dominant band at 500 bp.

obtained (Fig. 1*A*, *right panel*). In total, 56% of pTRE2-511 clones and 72% of pTRE2-EGFP clones were stably transfected.

RT-PCR was conducted with total RNA prepared from clones that showed stable integration of the respective plasmids during genomic PCR. To analyze for inducibility, clones were cultured in the absence or presence of doxycyclin (1 μg/ml) for 2 days. Seven clones expressing antisense mRNA were obtained for pTRE2-511, and five clones for pTRE2-EGFP. Unfortunately, in almost all cases, no inducibility was found as exemplified for clone pTRE2-511#25 (Fig. 1*B*, *left panel*) and the clones pTRE2-EGFP#E2 and #E4 (Fig. 1*B*, *right panel*). However, since all clones were growing at reasonable rates, our initial concern that permanent suppression of RyR expression might be cytotoxic and thus that the cells might not be sufficiently expandable turned out not to be a serious problem. Thus, for further detailed characterization, only a few clones were selected: type 3 RyR antisense clone pTRE2-511#25 and control clones pTRE2-EGFP#E1 and #E2.

SDS-PAGE and Western blot analysis of clone pTRE2-511#25 revealed a greatly reduced expression of RyR as compared with the parent Tet-On Jurkat cell and with the control clones pTRE2-EGFP#E1 (Fig. 2) and pTRE2-EGFP#E2 (data not shown). In contrast, there was no change in expression of the IP_3R (Fig. 2), suggesting that expression of other proteins essentially involved in Ca^{2+} signaling was not altered by transfection with pTRE2 plasmids.

TCR/CD3 complex-mediated Ca^{2+} signaling was first analyzed in cell suspension in a dual-wavelength spectrophotometer (Table I and Fig. 3). The basal $[Ca^{2+}]_i$ was slightly but not significantly elevated in the clones pTRE2-511#25, pTRE2-EGFP#E1, and #E2 (Table I), indicating that the Ca^{2+} clearance mechanisms of the cells, *e.g.* the Ca^{2+} pumps of the endoplasmic reticulum and the plasma membrane, were unaltered by the transfection process. Upon stimulation with anti-CD3 monoclonal antibody OKT3, the parent Tet-On Jurkat T

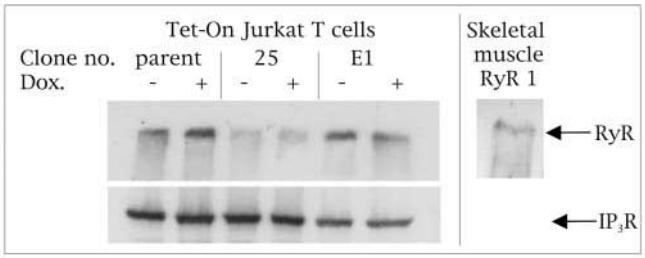

FIG. 2. **Western blot analysis of expression of RyR and IP_3R.** Parent Jurkat Tet-On Jurkat cells and clones pTRE2-511#25 and pTRE2-EGFP#E1 were homogenized, and P10 membranes were prepared as described under "Experimental Procedures." Protein (50 μg/lane) was separated on reducing SDS-PAGE (3% stacking, 6% separating gel). The proteins were tank-blotted (see "Experimental Procedures") onto a nitrocellulose membrane. This membrane was cut into two pieces according to the relative position of RyR and IP_3R. The channels were made visible by incubation with specific primary antibodies followed by secondary, horseradish peroxidase-conjugated goat anti-mouse antiserum using the ECL system (Amersham Biosciences) according to the manufacturer's protocol. Lanes marked with *Dox* and + indicate that the cells had been cultured in the presence of doxycyclin (1 μg/ml) for 6 days before preparation of P10 membranes. For comparison of protein mass, type 1 RyR highly purified from heavy sarcoplasmic reticulum of rabbit muscle (kind gift of Prof. M. Hohenegger, Vienna, Austria) was analyzed in parallel.

TABLE I

Basal global $[Ca^{2+}]_i$ in the different Tet-On Jurkat T cell clones

$[Ca^{2+}]_i$ was determined in Fura2-loaded cell suspensions as described in Fig. 3. Data are mean ± S.D. *dox* marks cells cultured in the presence of doxycycline (1 μg/ml) for 6 days.

Clone	Tet-On parent	pTRE2-511#25	pTRE-EGFP#E1	pTRE-EGFP#E2
$[Ca^{2+}]_i$ [nM]	43 ± 13 (n=20)	55 ± 16 (n=9)	52 ± 19 (n=13)	52 ± 16 (n=11)
$[Ca^{2+}]_i$ [nM]/dox	43 ± 15 (n=11)	57 ± 17 (n=8)	53 ± 16 (n=13)	50 ± 14 (n=11)

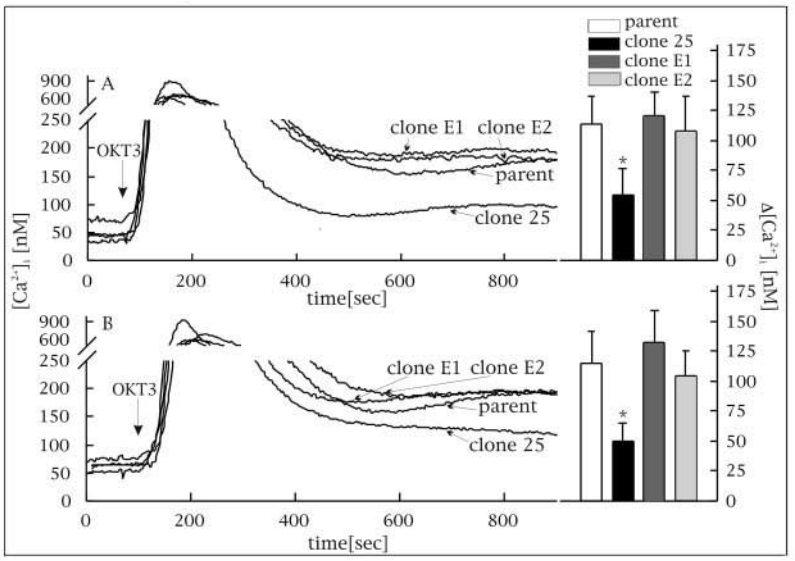

FIG. 3. **Analysis of TCR/CD3 complex-mediated global Ca^{2+} signaling in type 3 RyR-deficient Jurkat T cells.** The cells were incubated (*B*) or not (*A*) in the presence of doxycyclin (1 μg/ml) for 6 days. Then, the cells were loaded with Fura2-AM as described (13). $[Ca^{2+}]_i$ was then determined in aliquots of 1.5×10^6 cells in a Hitachi F-2000 spectrofluorimeter operated in the ratio mode (alternating excitation wavelengths, 340 and 380 nm; emission wavelength, 495 nm). Each tracing was calibrated for the maximal and minimal ratio at the end of the measurement. *Panels* on the *left side* of *A* and *B* show typical tracings obtained with the different cell clones. *Panels* on the *right side* of *A* and *B* summarize the data of the plateau phase at 900 s with corresponding basal values subtracted (mean ± S.D., n = 8 to 20). The *asterisk* indicates significant statistical differences *versus* parent and control clones according to the Student's t test ($p \leq 0.05$).

cells and all clones showed the typical biphasic pattern of Ca^{2+} signaling (17). Most importantly, the sustained Ca^{2+} signal of the type 3 RyR antisense clone pTRE2-511#25 was significantly reduced as compared with the parent Tet-On Jurkat T cell or with control clones pTRE2-EGFP#E1 and #E2 (Fig. 3). In accordance with suppression of type 3 RyR expression already occurring without induction by doxycyclin (Fig. 2), there was no difference between cells preincubated without (Fig. 3*A*) or with doxycyclin (Fig. 3*B*). A second TET-On Jurkat T cell clone stably transfected with a different antisense construct against the type 3 RyR showed a similar reduction of the sustained Ca^{2+} signal (data not shown). These data suggest that the type 3 RyR is involved in the sustained phase of T cell Ca^{2+} signaling. In contrast, the initial rapid Ca^{2+} peak was not different between the different clones, except for a slightly increased Ca^{2+} peak in clone pTRE2-EGFP#E1.

Confocal Ca^{2+} imaging was then applied to analyze TCR/CD3 complex-mediated Ca^{2+} signaling on the subcellular level. A deconvolution-based confocal Ca^{2+} imaging technique was recently developed in our laboratory and applied to the analysis of pacemaking subcellular Ca^{2+} signals that appear between stimulation and the first global Ca^{2+} signal in Jurkat T cells.[2] In the current study, a modified protocol was used for the first time to analyze subcellular Ca^{2+} signals at a much later time point, *e.g.* in the sustained phase where a significant difference between the type 3 RyR antisense clone pTRE2-511#25 and the control clones pTRE2-EGFP#E1 and #E2 was already observed in cell suspension (Fig. 3). Stimulation of both clone pTRE2-EGFP#E1 and clone pTRE2-511#25 by solid-phase bound OKT3 activated a rapid, global, and high Ca^{2+} response in almost all cells (Fig. 4, *A* and *D*). However, as already seen in suspension (Fig. 3), there was a significantly reduced phase of sustained Ca^{2+} signaling in type 3 RyR antisense clone pTRE2-511#25 as compared with control clone pTRE2-EGFP#E1 (Fig. 4, *A* and *D*). Analysis of the subcellular Ca^{2+} signals of two single cells (Fig. 4, *A* and *D*, *red lines*) representative of the average of clone pTRE2-511#25 and clone pTRE2-EGFP#E1 (Fig. 4, *A* and *D*, *green lines*) revealed a drastically reduced number of individual Ca^{2+} signals with amplitudes >115 nM (Fig. 4, *B* and *E*, *dotted lines* in *C* and *F*). Most importantly, both the total number and the amplitudes of the subcellular Ca^{2+} signals in three different regions of the cell were significantly lower for clone pTRE2-511#25 as compared with clone pTRE2-EGFP#E1 (Fig. 4, *C* and *F*). These data represent the first characterization of subcellular Ca^{2+} signals in type 3 RyR-deficient T cells and demonstrate that the type 3 RyR is necessary for amplification of local Ca^{2+} signals during the sustained phase of T cell Ca^{2+} signaling.

Since evidence has been presented that the type 3 RyR is the target Ca^{2+} channel for the calcium-mobilizing second messenger cADPR (2), permeabilized cells were prepared, and the Ca^{2+}-releasing effect of cADPR and IP_3 was analyzed. Fig. 5 (*left panel*) shows typical Ca^{2+} release tracings obtained by addition of 10 μM cADPR in the type 3 RyR antisense clone pTRE2-511#25 as compared with the parent Tet-On Jurkat T cell and the control clone pTRE2-EGFP#E1. The response to cADPR was significantly reduced, whereas IP_3 released Ca^{2+} at a similar magnitude in the three different clones (Fig. 5, *right panel*). These data demonstrate directly that knock-down of the type 3 RyR significantly decreases the Ca^{2+}-mobilizing effect of cADPR.

DISCUSSION

In the current study, we have generated a novel, stably transfected Jurkat T cell clone with greatly reduced expression of the type 3 RyR as shown by Western blot analysis. Stable integration of the antisense plasmid was demonstrated by genomic PCR, and expression of antisense mRNA was demonstrated by RT-PCR. The clone was successfully used to analyze the role of type 3 RyR in TCR/CD3 complex-mediated Ca^{2+} signaling. Reduced expression of the type 3 RyR resulted in significantly decreased Ca^{2+} signaling in the sustained phase

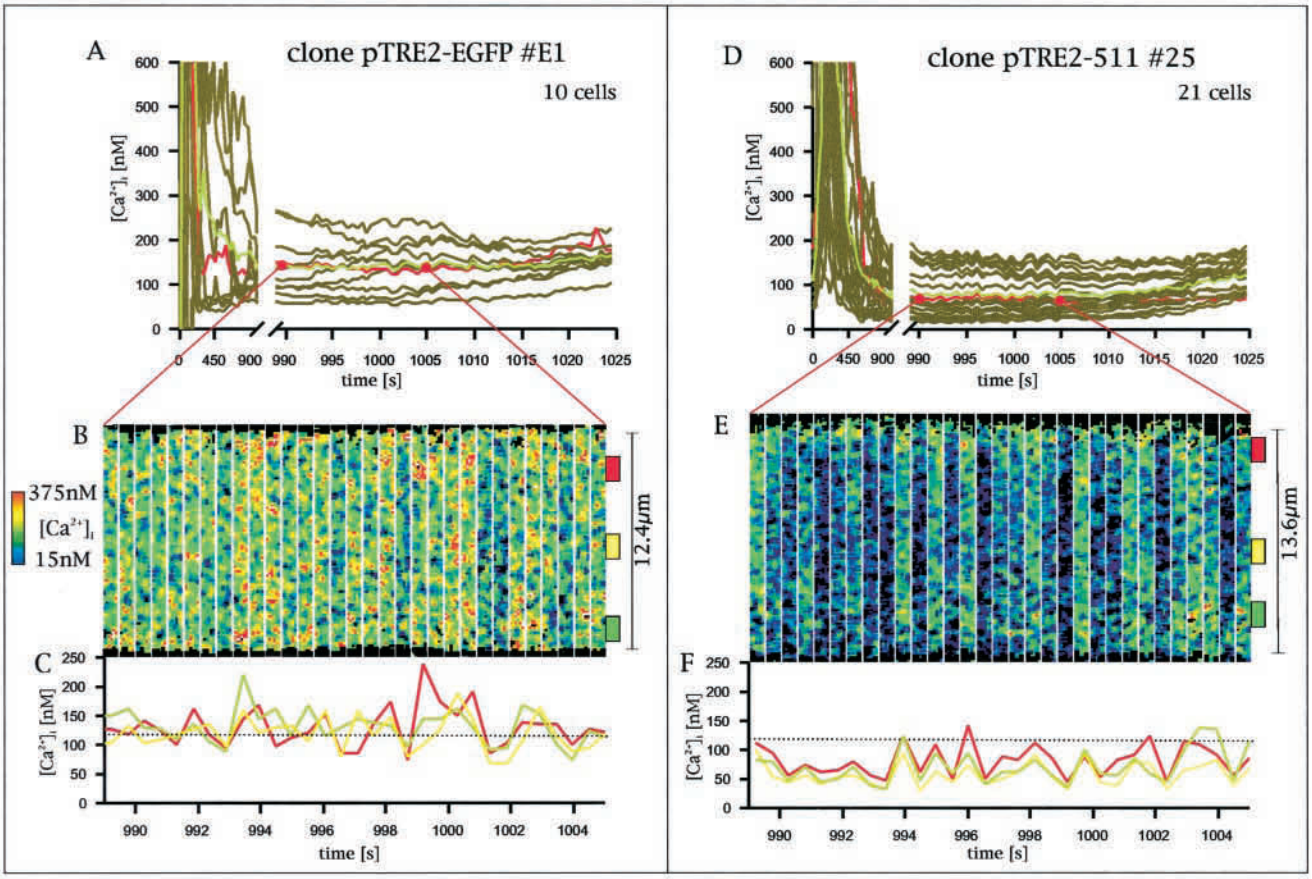

FIG. 4. **Analysis of TCR/CD3 complex-mediated local Ca^{2+} signaling in type 3 RyR-deficient Jurkat T cells.** The cells were loaded with Fura2-AM as described under "Experimental Procedures." Confocal Ca^{2+} imaging was carried out as described under "Experimental Procedures." The cells, either control clone pTRE2-EGFP#E1 or type 3 RyR antisense clone pTRE2-511#25, were placed on the stage of the confocal imaging system in a small chamber mounted on thin glass coverslips coated with anti-CD3 monoclonal antibody OKT3. Acquisition of images was started immediately at a slow rate (2 confocal ratios/min) until 980 s; then, images were acquired at maximal rate (2 confocal ratios/sec). *A* and *D*, the mean $[Ca^{2+}]_i$ of whole cells observed over time. The *green lines* show the average Ca^{2+} signal, whereas the *red lines* highlight two individual cells representative of these calculated averages. *B* and *E*, line scans spanning from edge to edge of these representative cells. Amplitudes from selected regions (indicated by *colored boxes* in *B* and *E*) of these two representative cells are shown in *C* and *F*.

and a significantly impaired response toward cADPR but not IP_3. For the first time, the role of the type 3 RyR in sustained Ca^{2+} signaling was directly visualized as a significant contribution to the number and the magnitude of subcellular Ca^{2+} signals.

Although complementary RNA and DNA have been widely used for gene silencing, the mechanisms underlying these antisense approaches were not well understood (reviewed in Ref. 21). However, the discoveries that (i) double-stranded RNA was a better gene silencer than antisense RNA (23), (ii) double-stranded RNA is cleaved to small interfering RNA (24), and (iii) such small interfering RNA then activates specific digest of the original mRNA by the so-called RNA-induced silencing complex (RISC) (27) likely suggest that the antisense RNA acts via small interfering RNA. For intracellular Ca^{2+} channels, different antisense approaches have been used. Macrez and co-workers (20) injected chemically modified (phosphorothioate) antisense DNA oligomers directed toward each single subtype of RyR into single rat portal vein myocytes in primary culture, and after a few days, they analyzed the efficacy of their antisense approach by RT-PCR and staining of single cells by BODIPY FL-X ryanodine. Knock-down of both type 1 and type 2 RyR efficiently decreased local and global Ca^{2+} responses activated by membrane depolarization or angiotensin II, whereas caffeine-activated global Ca^{2+} signaling was only par-

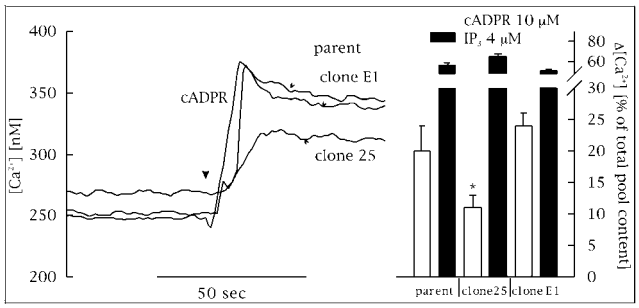

FIG. 5. **Analysis of Ca^{2+} release by cADPR and IP_3 in type 3 RyR-deficient Jurkat T cells.** Permeabilized cells were prepared, and $[Ca^{2+}]$ was determined in the presence of Fura2, ATP, an ATP-regenerating system in a Hitachi F-2000 spectrofluorimeter operated in the ratio mode (alternating excitation wavelengths, 340 and 380 nm; emission wavelength, 495 nm) as described recently (34). The *left panel* shows characteristic tracings from permeabilized cell suspensions of the parent Tet-On Jurkat cell, control clone pTRE2-EGFP#E1, or type 3 RyR antisense clone pTRE2-511#25 responding to 10 μM cADPR. The *right panel* summarizes data obtained upon successive additions of 10 μM cADPR, 4 μM IP_3, and 1 μM ionomycin. Data are expressed as percent of total pool content (sum of Ca^{2+} release by 10 μM cADPR, 4 μM IP_3, and 1 μM ionomycin) and are presented as mean ± S.E., $n = 3$ to 7). The *asterisk* indicates significant statistical differences *versus* parent ($p = 0.081$) and control clone pTRE2-EGFP#E1 ($p \leq 0.05$) according to the Student's *t* test.

tially reduced (20). Interestingly, knock-down of type 3 RyR had no effect on these activation pathways (20). However, under conditions of Ca^{2+} overload, type 3 RyR was activated by caffeine or local increases in $[Ca^{2+}]_i$ (28). These impressive studies showed for the first time by a molecular approach the function of the different RyR subtypes in portal vein smooth muscle cells. However, a disadvantage of the experimental strategy of Macrez and co-workers (20) was that only a limited number of cells could be injected with antisense oligomers, making Western blot analysis of the proteins impossible. In addition, no stable cell lines were established, requiring repeated laborious injections of antisense oligomers. A different approach toward the IP_3R was carried out by Marks and colleagues (19): Jurkat T cells were stably expressed with a vector, allowing for constitutive expression (pREP10) containing a fragment of the human type 1 IP_3R in antisense orientation. Although the proliferation rate of these cells decreased by about 75%, it was impressively demonstrated that deletion of the IP_3R almost completely impaired TCR/CD3-mediated Ca^{2+} signaling but not capacitative Ca^{2+} signaling activated by the sarcoplasmic/endoplasmic reticular Ca^{2+} ATPase inhibitor thapsigargin (19). These important results suggest that (i) the whole machinery of T cell Ca^{2+} signaling depends on rapid, IP_3-mediated Ca^{2+} release in the first minutes of T cell activation and that (ii) additional Ca^{2+} channels are present in Jurkat T cells allowing for passive Ca^{2+} leak from the endoplasmic reticulum in case of thapsigargin stimulation. Both results were confirmed recently: microinjection of the IP_3 antagonist D-*myo*-inositol 1,4,6-phosphorothioate before TCR/CD3 stimulation completely abolished Ca^{2+} signaling (2), whereas microinjection a few minutes after the first Ca^{2+} spike had no effect (2), confirming that IP_3 acts to deliver the first global Ca^{2+} responses, which are then used as co-activators of the subsequent systems. Secondly, the expression of additional intracellular Ca^{2+} release channels that would carry the leak current from the endoplasmic reticulum of type 1 IP_3R-deficient cells in case of sarcoplasmic/endoplasmic reticular Ca^{2+} ATPase inhibition was demonstrated: on the one hand, the expression of types 2 and 3 IP_3R was almost unaltered by the type 1 IP_3R-specific antisense construct (29), and on the other hand, sufficient evidence for RyR expression in Jurkat T cells has been obtained in the meantime (2, 10–18).

Importantly, Jayaraman and Marks (29) showed that although the type 1 IP_3R antisense cDNA had at least 60% identity with types 2 and 3 IP_3R, there was almost no effect on the protein expression of these additional IP_3R isoforms. In our study, the type 3 RyR antisense fragment used had a homology of only about 29% to the types 1 and 2 RyR, assuring that any interference with expression of these other RyR subtypes could be excluded.

The data presented in this study suggest that the type 3 RyR plays an essential role as a Ca^{2+} release system in the sustained phase of TCR/CD3-mediated Ca^{2+} signaling. The fact that cADPR is elevated during this phase (2) and that the membrane-permeant cADPR antagonist 7-deaza-8-Br-cADPR decreased Ca^{2+} signaling in this phase (2) indicates that during sustained Ca^{2+} signaling, cADPR controls CICR via the type 3 RyR. Our confocal Ca^{2+} imaging data (Fig. 4) demonstrate directly that in cells with largely reduced expression of the type 3 RyR, the subcellular Ca^{2+} release events are much smaller and less abundant as compared with the control cells, indicating that cADPR-controlled CICR acts as an amplification system to increase the magnitude of the sustained Ca^{2+} response. The fact that the sustained Ca^{2+} signal in T cells requires permanent Ca^{2+} entry can be easily connected to our model: first, we have shown previously that microinjection of cADPR into Jurkat T cells activates sustained Ca^{2+} entry (30), and secondly, it was shown recently that in IP_3R-deficient DT40 cells that express types 1 and 3 RyR, capacitative Ca^{2+} entry was regulated by these RyR subtypes and cADPR (31).

Since no complete knock-out of type 3 RyR expression could be achieved in our experimental model, the remaining Ca^{2+} signal in intact T cells (Fig. 3), but also in permeabilized T cells stimulated by cADPR (Fig. 5), may be due to residual type 3 RyR expression, but more likely, additional systems, such as the IP_3R system in intact cells or additional cADPR-sensitive Ca^{2+} channels may be involved. Similarly, in muscles from type 3 $RyR^{-/-}$ mice, effects of cADPR could be still detected and were explained by an effect of cADPR on the type 1 RyR (32). However, it is remarkable that three different ways to interfere with the cADPR/RyR signaling pathway in Jurkat T cells, namely (i) cADPR antagonism (2), (ii) inhibition of ADP-ribosyl cyclase activity,[3] and (iii) knock-down of the type 3 RyR, resulted in a very similar reduction (around 50%) on the long-lasting global Ca^{2+} signal.

In conclusion, we have generated and characterized a novel Jurkat T cell line with greatly reduced expression of the type 3 RyR. Analysis of TCR/CD3-mediated Ca^{2+} signaling in cell suspensions and on the subcellular level indicate that during sustained Ca^{2+} signaling, cADPR controls CICR via the type 3 RyR by significant amplification of local Ca^{2+} signals.

Acknowledgments—We are grateful to Prof. Martin Hohenegger, University of Vienna, for a gift of purified skeletal muscle ryanodine receptor and to Martin Kalkstein and Sandra Frederichs for expert technical assistance.

REFERENCES

1. Guse, A. H., and Emmrich, F. (1991) *J. Biol. Chem.* **266,** 24498–24502
2. Guse, A. H., da Silva, C. P., Berg, I., Skapenko, A. L., Weber, K., Heyer, P., Hohenegger, M., Ashamu, G. A., Schulze-Koops, H., Potter, B. V. L., and Mayr, G. W. (1999) *Nature* **389,** 70–73
3. da Silva, C. P., and Guse, A. H. (2000) *Biochim. Biophys. Acta* **1498,** 122–133
4. Berg, I., Potter, B. V. L., Mayr, G. W., and Guse, A. H. (2000) *J. Cell Biol.* **150,** 581–588
5. Sethi, J. K., Empson, R. M., Bailey, V. C., Potter, B. V. L., and Galione, A. (1997) *J. Biol. Chem.* **272,** 16358–16363
6. Schöttelndreier, H., Mayr, G. W., and Guse, A. H. (2001) *Cell. Signal.* **13,** 895–899
7. Guse, A. H. (2002) *Curr. Mol. Med.* **2,** 273–282
8. Galione, A., Lee, H. C., and Busa, W. B. (1991) *Science* **253,** 1143–1146
9. Lee, H. C. (2001) *Annu. Rev. Pharmacol. Toxicol.* **41,** 317–345
10. Bourguignon, L. Y., Chu, A., Jin, H., and Brandt, N. R. (1995) *J. Biol. Chem.* **270,** 17917–17922
11. Ricard, I., Martel, J., Dupuis, L., Dupuis, G., and Payet, M. D. (1997) *Cell. Signal.* **9,** 197–206
12. Guse, A. H., Tsygankov, A. Y., Weber, K., and Mayr, G. W. (2001) *J. Biol. Chem.* **276,** 34722–34727
13. Guse, A. H., Roth, E., and Emmrich, F. (1993) *Biochem. J.* **291,** 447–451
14. Hohenegger, M., Berg, I., Weigl, L., Mayr, G. W., Potter, B. V. L., and Guse, A. H. (1999) *Br. J. Pharmacol.* **128,** 1235–1240
15. Guse, A. H., da Silva, C. P., Emmrich, F., Ashamu, G. A., Potter, B. V. L., and Mayr, G. W. (1995) *J. Immunol.* **155,** 3353–3359
16. Guse, A. H., da Silva, C. P., Weber, K., Ashamu, G. A., Potter, B. V. L., and Mayr, G. W. (1996) *J. Biol. Chem.* **271,** 23946–23953
17. Guse, A. H. (2002) in *Cyclic ADP-ribose and NAADP: structures, metabolism and functions* (Lee, H. C., ed), Kluwer Academic Publishers, Dordrecht, in press
18. Hakamata, Y., Nishimura, S., Nakai, J., Nakashima, Y., Kita, T., and Imoto, K. (1994) *FEBS Lett.* **352,** 206–210
19. Jayaraman, T., Ondriasova, E., Ondrias, K., Harnick, D. J., and Marks, A. R. (1995) *Proc. Natl. Acad. Sci. U. S. A.* **92,** 6007–6011
20. Coussin, F., Macrez, N., Morel, J.-L., and Mironneau, J. (2000) *J. Biol. Chem.* **275,** 9596–9603
21. Nellen, W., and Liechtenstein, C. (1993) *Trends Biochem. Sci.* **18,** 419–423
22. Novottny, J., Diegel, S., Schirmacher, H., Mohrle, A., Hildebrandt, M., Oberstrass, J., and Nellen, W. (2001) *Methods Enzymol.* **342,** 193–212
23. Fire, A., Xu, S., Montgomery, M. K., Kostas, S. A., Driver, S. E., and Mello C. C. (1998) *Nature* **391,** 806–811
24. Elbashir, S., Lendeckel, W., and Tuschl, W. (2001) *Genes Dev.* **15,** 188–200
25. Bernstein, E., Caudy, A. A., Hammond, S. M., and Hannon, G. J. (2001) *Nature* **409,** 363–366
26. Gossen, M., Freundlieb, S., Bender, G., Muller, G., Hillen, W., and Bujard, H.

[3] K. Schweitzer, B. V. L. Potter, and A. H. Guse, unpublished data.

(1995) *Science* **268,** 1766–1769
27. Hammond, S. M., Bernstein, E., Beach, D., and Hannon, G. J. (2000) *Nature* **404,** 293–296
28. Mironneau, J., Coussin, F., Jeyakumar, L. H., Fleischer, S., Mironneau, C., and Macrez, N. (2001) *J. Biol. Chem.* **276,** 11257–11264
29. Jayaraman, T., and Marks, A. R. (1997) *Mol. Cell. Biol.* **17,** 3005–3012
30. Guse, A. H., Berg, I., da Silva, C. P., Potter, B. V. L., and Mayr, G. W. (1997) *J. Biol. Chem.* **272,** 8546–8550
31. Kiselyov, K., Shin, D. M., Shcheynikov, N., Kurosaki, T., and Muallem, S. (2001) *Biochem. J.* **360,** 17–22
32. Fulceri, R., Rossi, R., Bottinelli, R., Conti, A., Intravaia, E., Galione, A., Benedetti, A., Sorrentino, V., and Reggiani, C. (2001) *Biochem. Biophys. Res. Commun.* **288,** 697–702
33. Schweitzer, K., Mayr, G. W., and Guse, A. H. (2001) *Anal. Biochem.* **15,** 218–226
34. Guse, A. H., Cakir-Kiefer, C., Fukuoka, M., Shuto, S., Weber, K., Bailey, V. C., Matsuda, A., Mayr, G. W., Oppenheimer, N., Schuber, F., and Potter, B. V. L. (2002) *Biochemistry* **41,** 6744–6751